Chalcogenide Letters Vol. 16, No. 9, September 2019, p. 425 - 431

SYNTHESIS AND TRIBOLOGICAL PERFORMANCE OF Cu-BASED COMPOSITES WITH $MoSe_2$/MoOx(x=2,3)

M. Q. XUE*, D. Q. LIU, K. Q.HAN
Changzhou Institute of Industry Technology, Changzhou, Jiangsu 213164, P. R. China

In this study, nano structure $MoSe_2$/MoOx(x=2,3) powders were fabricated, and the corresponding Cu-based composites (Cu/$MoSe_2$/MoOx(x=2,3)) were obtained by powder metallurgy technique. The phase compositions and morphology of Cu-based composites were measured by scanning electronic microscope, optical microscope, X-ray diffraction and their tribological properties were investigated by ball-on-disc NANOVEA Micro Tribometer. The results show that the addition of $MoSe_2$/MoOx improves the friction-reducing and anti-wear properties of copper matrix. The excellent tribological performance is attributed to the synergic effects of the $MoSe_2$/MoOx in the nanocomposite structure.

(Received March 12, 2019; Accepted September 2, 2019)

Keywords: $MoSe_2$/MoOx, Cu-based composites, Phase composition, Friction, Wear

1. Introduction

Metal matrix composites have attracted much attention in the past decades due to their special properties such as high specific strength and stiffness, high abrasion resistance, strong corrosion resistance and large elastic modulus [1]. Therefore, it has been reported in the literature that the addition of solid lubrication particles into the metal matrix not only improves the anti-wear performance of the material, but also improves the wear performance and self-lubrication performance of the material. Lead was once considered to be the best self-solid lubricant. Due to its harmful effects, the use of lead was restricted, which prompted researchers to look for alternative materials to guarantee the tribological properties similar to lead [2].

Copper matrix composites have been widely used in the fields of aerospace electronic components, automotive machinery and other fields because they not only maintain the high electrical conductivity and thermal conductivity of copper and excellent process performance, but also have high strength and excellent high temperature performance [3-4]. On this basis, Cu based transition metal dichalcogenides compounds were introduced and developed. Transition metal dichalcogenides have hexagonal layered structure, which has excellent self-lubricant property, so far, many attempts have been done to improve the mechanical and tribological properties of copper matrix by the means of adding various transition metal dichalcogenides. Kumar et al. [5] have investigated the tribological and mechanical properties of MoS_2 reinforced copper alloy composites, and found that the obtained copper alloy composites show higher hardness and lower wear rates. Tang et al. [6-8] have prepared copper matrix composites using copper powders and $NbSe_2$, and found that the appropriate contents of $NbSe_2$ in composites improving the tribological properties effectively. Xu et al. [9] tested tribological properties of Cu-doped WS_2 films, and a lower wear rate and longer wear life performance was obtained. Kovalchenko et al.[10] also reported the fabrication and tribological properties of copper by the incorporation of MoS_2 and $MoSe_2$, and presented some of its mechanical and wear mechanisms.

Therefore, the solvothermal subsequent calcination method was employed in this work to synthesize nano $MoSe_2$/MoOx, Cu-based composites with $MoSe_2$/MoOx were successfully fabricated by means of powder metallurgy (P/M) method. The tribological behavior of the

*Corresponding author: xuemaoq@163.com

Cu-based composites with $MoSe_2/MoOx$ was investigated by a ball-on-disc tribotester. This objective of this paper is to explore the potential of nano $MoSe_2/MoOx$ to serve as filler of copper matrix composites.

2. Experimental details

2.1. Materials and physical techniques

All starting reagents, including selenium powder, sodium molybdate dihydrate ($Na_2MoO_4 \cdot 2H_2O$) and hydrazine hydrate ($N_2H_4 \cdot H_2O$) were purchased from Sinopharm (Shanghai) Chemical Reagent Co., Ltd. and used as received. Mechanical stirring was carried out in a magnetic stirrer. X-ray powder diffraction (XRD) measurements were performed using a Shimadzu LabX XRD-6000 diffractometer with Cu-Kα radiation. X-ray data were analyzed by using the Jade software. The samples were characterized by scanning electron microscope (SEM) JEOL JXA-840A and energy-dispersive spectrometer (EDS). The friction coefficient was recorded automatically by a computer. The microstructure and wear scar of copper matrix composites were observed using optical microscope. Morphologies of worn surface were measured on a PS50 non-contact optical profile testing instrument (NANOVEA Inc., USA).

2.2. Synthesis

A mixture of 0.483 g $Na_2MoO_4 \cdot 2H_2O$ and 0.316 g Se powder were dissolved in 70 mL hydrazine hydrate ($N_2H_4 \cdot H_2O$) and deionized water under constant stirring. The mixture was then placed in a Teflon reactor and heated at 200 °C for 48h. The resulting black powder was isolated by centrifugation, washed with distilled water and absolute ethanol and dried at 80℃, then calcined in a nitrogen atmosphere at 550°C for 30min. After gradual cooling of samples, $MoSe_2/MoOx$ (x=2,3) particles were obtained.

The samples of Cu/ $MoSe_2/MoOx$ composites used in this study were made by powder metallurgy (P/M). The powders of copper and $MoSe_2/MoOx$ in the weight ratio of 14:1 were mixed mechanically. Then the mixed powders were cold compressed under the pressure of 200 MPa and sintered at 850℃ for 2h. under vacuum. After naturally cooled to room temperature, the copper-based composites were generated. Pure copper samples were also prepared by powder metallurgy for comparison.

2.3. Tribological tests procedure

Tribological properties were evaluated with a NANOVEA Micro Tribometer under dry conditions and in an air atmosphere. The balls used were 440C stainless steel had a 10.0 mm in diameter with a hardness of 62 HRC. The disc specimens were Cu/$MoSe_2/MoOx$ composite disc (Ø 30 mm × 5 mm). The applied load was 1-7 N, and the sliding speed was 0.17 m/s. The wear scar widths were measured by a common optical microscope and non-contact optical profile testing instrument.

3. Results and discussion

3.1. Microstructure of $MoSe_2/MoOx$

The X-ray diffraction (XRD) pattern of $MoSe_2/MoOx$(x=2,3) nanocomposites is shown in Fig. 1(a). As seen in the XRD patterns, after heat treatment at 550°C in nitrogen atmosphere, the characteristic peaks of $MoSe_2$ were still obvious and became sharper, while a relatively strong characteristic peak of MoO_2 and MoO_3 can be found compared with before heat treatment [11].The results indicate that $MoSe_2/MoOx$(x=2,3) were successfully fabricated.

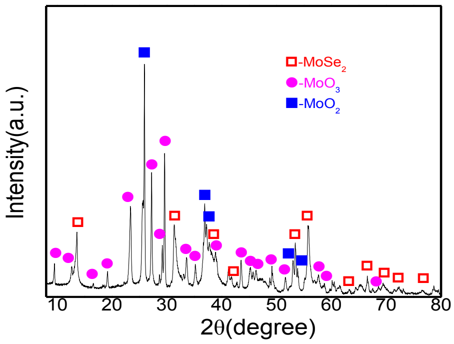

(a)

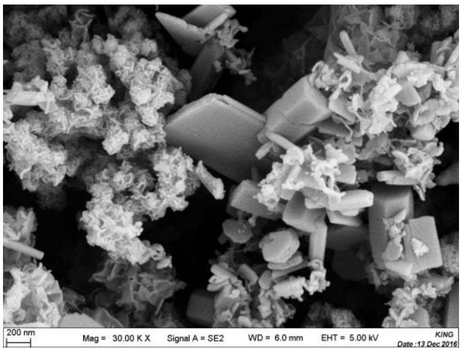

(b)

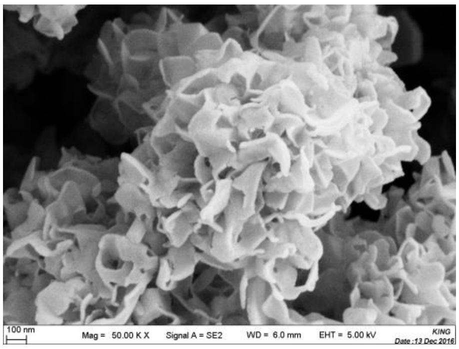

(c)

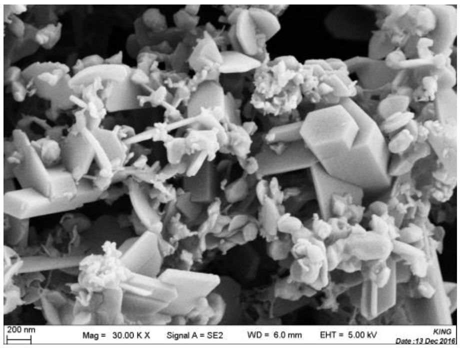

(d)

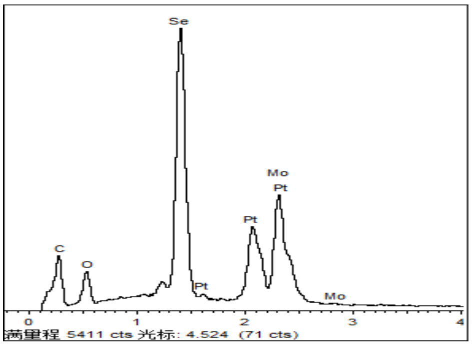

(e)

Fig. 1. (a) X-ray diffraction (XRD) pattern, (b)-(d) Scanning electron microscope (SEM) images and (e) Energy-dispersive spectrometer EDS of $MoSe_2/MoOx$.

Fig. 1(b)-(d) shows the scanning electron microscopy (SEM) images of $MoSe_2/MoOx$(x=2,3). It can be clearly seen from Fig. 1 (b) that nanomaterials composed of many aggregated particles, flakes and prisms. The magnified SEM image (Fig. 1(c), (d)) further gives the details of hybrid nanocomposite. Fig. 1(c), the high-magnification SEM image of nanoparticles, offer a clear view of the surface structure, it reveals that the entire structure of the architecture is built from several dozen twisted nanosheets with the thickness about 20 nm, these nanosheets were connected to each other through the center to form flowerlike structures. The SEM image with higher magnification of flakes and prisms in Fig. 1(d) shows that the thickness of the obtained flakes is 30-80 nm, small amount of hexagonal prism is about 300 nm in diameter. Besides, Energy-dispersive spectrometer (EDS) result as shown in Fig. 1(d) shows the powder consisted of element Mo, O and Se. From this, it was determined that the hybrid $MoSe_2/MoOx$(x=2,3) were fabricated.

3.2. Characterization, conductivity and microhardness of Cu-based composites

Fig. 2 (a) is the XRD patterns of Cu-based composites prepared by P/M. It was found that the diffraction peaks primarily belonged to the Cu phase. Some other peaks except Cu were observed in the XRD patterns of Cu-base composites, such as $MoSe_2$, MoO_2 and MoO_3 phases. Fig. 2 (b), (c) shows the microstructure of sintered copper and Cu-based composites which was been characterized by optical micrographs after metallographic preparation. It can be seen that the pure Cu is compact, the microstructures of $MoSe_2$/MoOx (x=2,3) showed good bonding of Cu particles, the $MoSe_2$/MoOx particles embedded in the matrix.

Conductivity was measured using an FQR-7501A eddy current conductometer. A load of 100 N and the duration time of 15 s were employed for microhardness measurement. Five tests were carried out at different places of composites and the mean value was given. The conductivity and microhardness of Cu-based composites is 17.2 MS/m and 103.5Hv.

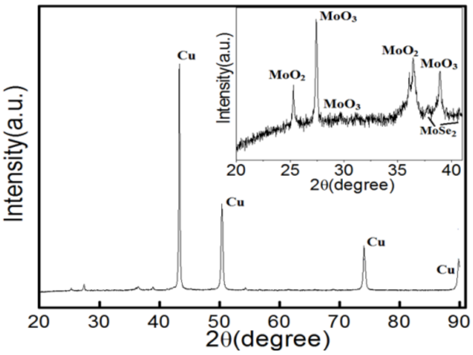

(a)

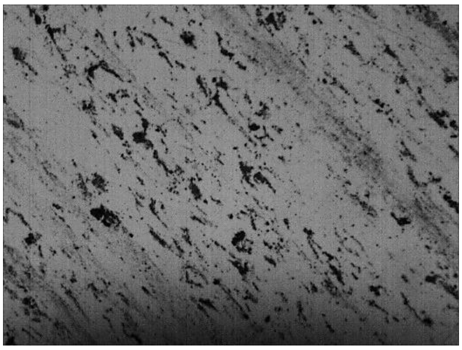

(b) *(c)*

Fig. 2. (a)XRD pattern and optical microscope image of (b) copper and (c) Cu-based composites with $MoSe_2$/MoOx.

3.3. Friction and wear behavior

The friction coefficients of copper and composites at sliding speeds 0.17 m/s with different loads are shown in Fig. 3. It can be seen in Fig. 3 (a) that after a slightly shorter running-in stage, the friction coefficients of copper became stable and almost remain constant from 0.32 to 0.45 with increasing normal load from 1N to 7N.

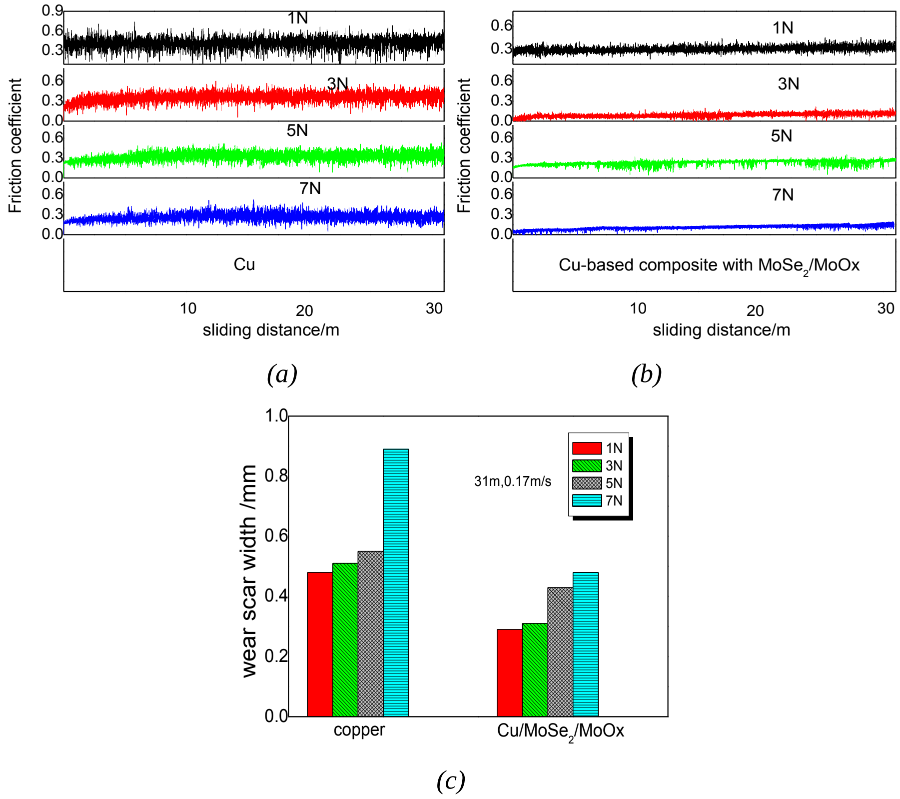

Fig. 3. Friction coefficient of (a) copper, (b) Cu/MoSe$_2$/MoOx composite and (c) wear scar width sliding against stainless steel balls under different normal loads.

The friction coefficient of Cu-based composite with MoSe$_2$/MoOx in Fig. 3(b) decreases with the increase of load, and their values are among the range of 0.11–0.31, is much lower than that of copper under the same load. The lowest friction coefficient is obtained when the load is 7 N. Under higher load, the temperature on the wear surface raises due to absorbing the heat transformed from the friction energy. The temperature increases with the load, at some point, it is even higher, which is called flash temperature is beneficial to the reduction of the friction coefficient.

Fig. 3(c) demonstrates the wear scar width versus normal loads at a rotation speed of 0.17m/s for copper and Cu-based composite with MoSe$_2$/MoOx. It can be observed that the wear scar width increases gradually with an increase in the applied load. The wear scar width of Cu added with MoSe$_2$/MoOx is lower than that of copper matrix material under same conditions. For copper, serious wear appears under load of 7N, while Cu-based composite with MoSe$_2$/MoOx shows excellent wear resistance. Therefore, it could be concluded that appropriate content of MoSe$_2$/MoOx could improve the tribological properties of Cu-based composites.

Fig. 4 illustrates microscopic images and noncontact three-dimensional morphologies of the wear scar on the disc after running for 31m under 7 N. The morphologies of the worn surface after friction tests are presented in Fig. 4(a) and (c). It can be seen in Fig. 4(a) that the wore surface of copper exhibits the characteristic of the typical abrasion accompanied with plastic deformation. During sliding process, the particles fall off and form a great deal of debris partially, and the rest adhere to the surface. The fall off debris makes the hardness are in significant discrepancy between friction pair materials, resulting in higher wear rate. The wore surface of Cu-based composite with MoSe$_2$/MoOx shown in Fig4 (c) is smooth and the scratches on the worn surfaces are slighter and more uniform.

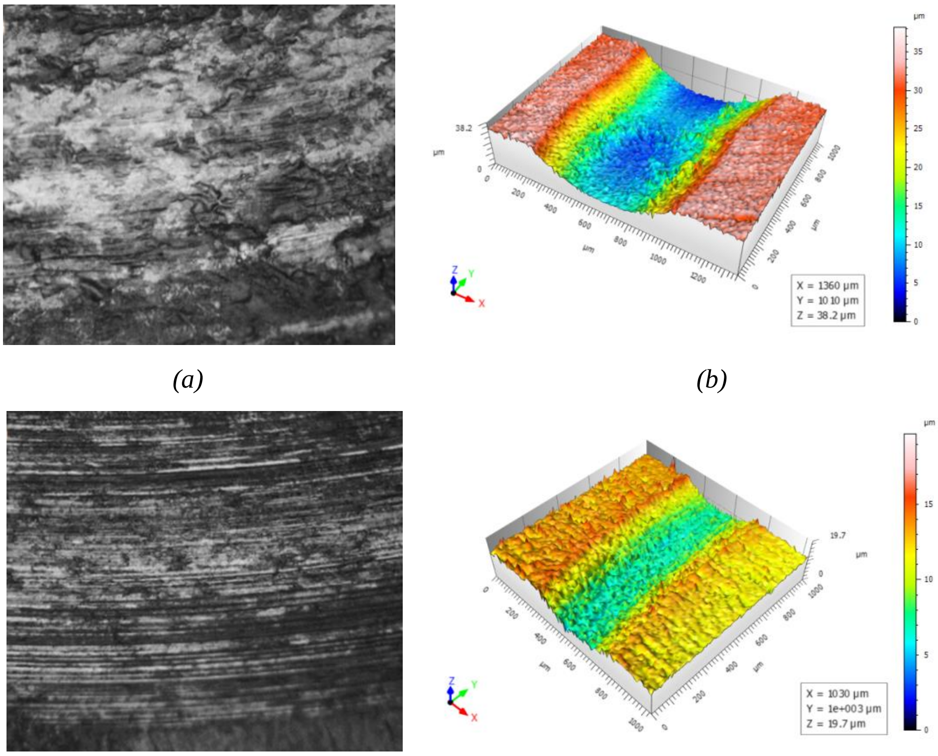

(a) (b)

(c) (d)

Fig. 4. Microscopic images and noncontact three-dimensional morphologies of the wear scar of (a)(b)copper, (c)(d) Cu/$MoSe_2$/MoOx composites after sliding against stainless steel ball

To further analyze the anti-wear performance of $MoSe_2$/MoOx, a PS50 non-contact optical profile testing instrument was used to investigate the wear surface morphology. Fig.4(b) and (d) presents the three-dimensional (3D) surface morphologies of the wear scar on the disc. As shown in Fig. 4(b), it can be clearly seen that the rubbing surface of copper is quite rough. On the contrary, the rubbing surface of Cu-based composite with $MoSe_2$/MoOx in Fig. 4(d) is smoother. Moreover, the depth and width of the wear scar for Cu-based composite with $MoSe_2$/MoOx is lower than that of copper. This further demonstrates that $MoSe_2$/MoOx can effectively improve the wear resistance of copper.

4. Conclusions

In this paper, a new type of Cu/$MoSe_2$/MoOx(x=2,3) composites was presented and their tribological properties were assessed. The main results and conclusions of this paper could be summarized as follows:

$MoSe_2$/MoOx were successfully fabricated by solvothermal subsequent calcination method, which was composed of $MoSe_2$ nano-flowers and MoOx nano flakes and prisms. Compared to copper matrix, copper-based composites with $MoSe_2$/MoOx had improved tribological properties. The excellent tribological performance is attributed to the synergic effects of the $MoSe_2$/MoOx in the nanocomposite structure.

Acknowledgments

The work was supported by the Enterprise practice training program for young teachers in higher vocational colleges of Jiangsu Province (2019QYSJPX037), 333 Project of Jiangsu Province (2016-7), Qinglan Project of Jiangsu (2017-15) and Key Program for Research Team of Changzhou Institute of Industry Technology (ZD201813101003).

References

[1] X. Zhang, C. Shi, E. Liu, F. He, L. Ma, Q. Li, Nanoscale **9**, 33 (2017).
[2] S. Singh, S. Gangwar, S. Yadav, Materials Today Proceedings **4**, 4 (2017).
[3] Y. Ming, W. Lin, H. Zhu, Scripta Materialia **138** (2017).
[4] B. Chen, S. Chen, J. Yang, Rare Metals **34**, 6 (2015).
[5] P. Senthil Kumar, K. Manisekar, E. Subramanian, Tribology Transactions **56**, 5 (2013).
[6] H. Tang, K. Cao, Q. Wu, Crystal Research and Technology **46**, 2 (2011).
[7] Q. Shi, J. Yang, W. Peng, RSC Advances **122**, 5 (2015).
[8] B. Chen, J. Yang, Q. Zhang, Materials & Design **75** (2015).
[9] S. Xu, X. Gao, M. Hu, Tribology Letters **55**, 1 (2014).
[10] A. M. Kovalchenko, O. I. Fushchich, S. Danyluk, Wear **290** (2012).
[11] X. Zhang, M. Xue, X. Yang, Micro & Nano Letters **10**, 7 (2015).